Chinese Science Bulletin 2004 Vol. 49 No. 6 542—546

In situ synthesis of TiC reinforced $Cu_{47}Ti_{34}Zr_{11}Ni_8$ bulk metallic glass composites

SUN Yufeng[1], ZHANG Guosheng[2], WEI Bingchen[1], LI Weihuo[1]& WANG Yuren[1]

1. National Microgravity Lab,Institute of Mechanics,Chinese Academy of Sciences (CAS),Beijing 100080,China;
2. Beijng Institute of Pharmaceutical Chemistry,Beijing 102205,China Correspondence should be addressed to Wang Yuren (e-mail: wangyr@imech.ac.cn)

Abstract ***In situ* Synthesized TiC particles and β-Ti dendrites reinforced $Cu_{47}Ti_{34}Zr_{11}Ni_8$ bulk metallic glass (BMG) composite ingots were preapared by the suction casting method. The ingots with diameters from 1 up to 4 mm were successfully obtained. It was shown that introducing TiC micro-sized particles into the amorphous matrix did not disturb the glass forming ability (GFA) of the matrix, while the yield strength and ductility could be well improved. The phase constitution, microstructure and elements distribution in the composites were studied by OM,XRD,SEM and EDS. It was shown that the *in situ* synthesized TiC particles acting as heterogeneous nulcleation sites promoted the precipitation of β-Ti dendrites, resulting in the formation of the TiC particles and β-Ti dendrites co-reinforced BMG composites. The compressive tests were employed to probe the yield strength and ductility of BMG composites.**

Keywords: bulk metallic glass, shear bands, *in situ* synthesis, composites.

DOI: 10.1360/03ww0180

BMGs have attracted much attention due to their excellent mechanical, magnetic and corrosion resistant properties. However, they have the key drawback of the inhomogeneous deformation in BMGs under the uniaxial loading. The formation and propagation of a few highly localized shear bands make the BMGs usually fail catastrophically and lose the bulk plasticity, which hinds the extensive application of BMGs as engineering materials[1,2]. To overcome the drawback of the low ductility of BMGs, one of commonly used methods is to introduce the uniformly distributed second phase particles into the BMG matrix to prevent the development and propagation of the highly localized shear bands. Another benefit of this method is that the second phase particles can promote the multiplication of shear bands. The existence of relatively large amount of shear banding under the uniaxial loading efficiently prevented the occurrence of inhomogeneous deformation, in the meanwhile did not influence the GFA of BMG matrix [3—5]. For instance, Johnson enhanced the compressive plasticity of $Zr_{41.25}Ti_{13.75}Cu_{12.5}Ni_{10}Be_{22.5}$ BMG composite to 18% by adding 40% volume fraction W filaments into the BMG matrix. Other Zr-based BMG composites reinforced by nano C-tube, C fiber, metal elements, *in-situ* precipitate or ductile dendrite have also been reported[6—10]. However, the problem is far from being well resolved for these kinds of composites. The metal elements in the BMG matrix may react with the nano C tubes or C fibers. The banded interface cannot be bonded tightly due to the large difference in physical properties between the high melting point metal element reinforcements and the amorphous matrix. The right chemical composition of the composite is strictly required when using *in situ* synthesized ductile phase as the reinforcement, while the size distribution and the amount of the precipitated particles are difficult to be controlled.

Zr-based BMG was commonly used as the matrix when preparing BMG composites, because it has better GFA than other family of BMG alloys. $Cu_{47}Ti_{34}Zr_{11}Ni_8$ BMG alloy was developed by Lin and Johnson and can be cast into at least 4 mm thick amorphous strips[11,12]. In this paper, we reported the thermal stability, phase constitution, microstructure and mechanical prosperities of the *in situ* synthesized TiC particles and ductile β-Ti dendrites reinforced $Cu_{47}Ti_{34}Zr_{11}Ni_8$ BMG composites prepared by suction cast in an arc furnace.

1 Experimental procedure

$Cu_{47}Ti_{34}Zr_{11}Ni_8$ BMG was chosen as the amorphous matrix. Cu, Ti, Zr and Ni metal elements with purity over 99.9% were used in preparation of the matrix alloy. The carbon powders used for *in situ* reaction were sieved by 320 meshes bolt. For the *in situ* synthesis of TiC particles, additional Ti elements with the Ti/C ratio of 1∶1 were added. The Ti-gathered arc furnace was used to produce master alloys in the protection of high purity Ar_2 gas. The master alloy was crashed into small fragments of different sizes. Thereafter, the alloy fragments were blended with C powder uniformly and remelted in the arc furnace for several times in order to induce the *in situ* Ti+C→TiC reaction completely performed. Such produced alloy ingots contained *in situ* synthesized TiC particles in the matrix. The alloy ingot was then crashed into fragments. The fragments were used for suction casting in the water-cooled Cu mold to produce ϕ1 mm, ϕ2 mm, ϕ3 mm and ϕ4 mm BMG composite cylinders with the weight fraction of *in situ* synthesized TiC particles at 1 wt.%, 3 wt.% and 5 wt.%, respectively.

The phase constitution of the samples was analyzed by Philips PW 1050 XRD diffractometer. The thermal analysis was performed with a Pekin-Elmer DSC 7 calorimeter at a heating rate of 0.33 K/s. A Jeol JSM-6400LV scanning electron microscopy (SEM) was used for the analysis of the morphologies of the as-casting cylinders and for characterization of fracture features. The sample for microstructure characterization was etched in the acid

solution of HF : HNO_3 : H_2O = 1 : 6 : 7. SEM electron microprobe analysis was used to determine the phase compositions. Room temperature compressive tests on cylindrical specimens with an aspect ration of 2 : 1 were done with a MTS793 mechanical testing device under quasi-static loading at a strain rate of 1×10^{-4}—1×10^{-3}/s.

2 Results and discussion

Figure 1 shows the XRD patterns of the $Cu_{47}Ti_{34}Zr_{11}Ni_8$ BMG composites. As expected, typical broad amorphous diffraction peak was shown for monolithic BMG cylinders when the diameter of the cylinder was under 3 mm. However, the fully amorphous feature of XRD profile can be kept for ϕ1—3 mm BMG composite samples containing 1 wt.% TiC particles. When the diameter of this kind BMG composite cylinder increased to ϕ4 mm, the crystalline diffraction peak superposed on the broad amorphous peak could be recognized, which came from the diffraction of β-Ti dendrite. In another aspect, when the amount of TiC particles increased up to 3 wt.%, broad amorphous peaks can only be observed for ϕ1 mm and ϕ2 mm cylinders, while some crystalline peaks can be recognized for the large cylinders with the diameters of ϕ3 mm and ϕ4 mm. When the amount of TiC particles increased up to 5 wt.%, the fully amorphous diffraction peak appeared only for ϕ 1mm BMG composite cylinders. The sharp crystalline diffraction peak could be observed for ϕ2 mm samples and the broad amorphous peak was vague for ϕ3 mm and ϕ4 mm samples.

Based on the above results, it was shown that the introducing of small amount of *in situ* TiC particles has no influence on the formation of BMG matrix, while might improve the GFA of BMG matrix due to the increase of the viscosity of the undercooled melt by the TiC particles.

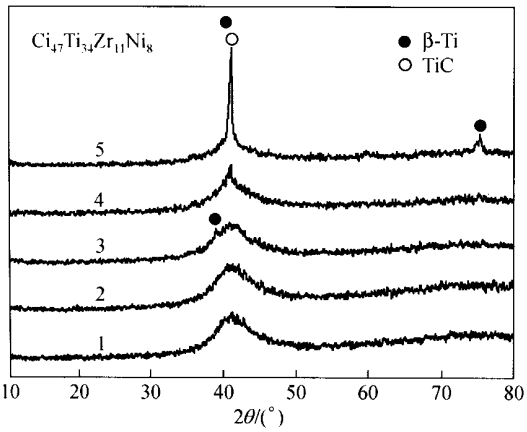

Fig. 1. XRD pattern of $Cu_{47}Ti_{34}Zr_{11}Ni_8$ BMG composites (x means the weight fraction of TiC in the composites). 1. x=0 wt.%, ϕ2 mm; 2, x=1 wt.%, ϕ2 mm; 3, x=1 wt.%, ϕ2 mm; 4, x=3 wt.%, ϕ3 mm, 5, x=5, wt.%, ϕ2 mm.

In another aspect, *in situ* synthesized TiC particles provided more heterogeneous nucleation sites for the nucleation of crystalline phase.

Figure 2 illustrates the DSC profiles of the ϕ1 mm composite and the corresponding monolithic samples. The glass transition and crystallization temperatures could be well recognized for both the composite sample and the monolithic BMG sample. The same DSC results were obtained for the composite samples of larger diameters of ϕ2 mm and ϕ3 mm. However, the glass transition temperature cannot be distinguished well on the DSC profile of ϕ4 mm composite sample. The undercooled liquid regions $\Delta T_x = T_x - T_g$ are listed in Table 1. As indicated by Table 1, ΔT_x increased no more via the increasing of the weight fraction of TiC particles from zero to 3 wt.%. This demonstrated that adding appropriate amount of TiC particles into the matrix did not lower the GFA, but could improve the thermal stability. When the amount of TiC increased to 5 wt.%, the undercooled liquid region shrank to be a narrow region due to more β-Ti dendrites precipitated from the melts. For ϕ3 mm composite sample containing 5 wt.% TiC particles, the volume fraction of BMG matrix decreased a lot and the glass transition temperature could not be found easily.

Table 1 Undercooled liquid region ΔT_x/K of the $Cu_{47}Ti_{34}Zr_{11}Ni_8$ BMG composites

ΔT_x/K	x = 0 wt.%	x = 1 wt.%	x = 3 wt.%	x = 5 wt.%
ϕ1 mm	58.06	61.45	64.47	61.5
ϕ2 mm	42.75	45.51	55.85	46.96
ϕ3 mm	40.06	41.39	48.9	–

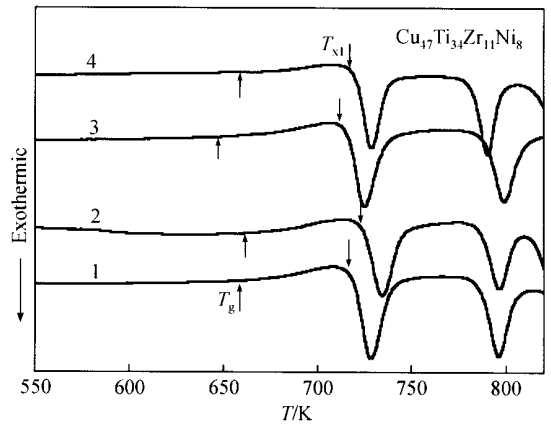

Fig. 2. DSC curves of the ϕ1 mm $Cu_{47}Ti_{34}Zr_{11}Ni_8$ BMG composites (x means the weight fraction of TiC in the composites). 1, x =5 wt.%; 2, x = 3 wt.%; 3, x = 1 wt.%; 4, x = 0 wt.%.

The microstructure characterization of the composite samples reveals that the β-Ti dendrites nucleate around the *in-situ* TiC particles and grow outward. EDS analysis shows that β-Ti dendrite is a solid solute and has a composition of 5.08 at.% Cu and 7.50 at.% Zr. The sizes of the

β-Ti dendrite increase via the diameter of the composite cylinder because of the lower cooling rate in solidification for large diameter composite cylinder. The number of the β-Ti dendrites in the composite cylinders at a fixed diameter increases with the increase of TiC weight fraction due to the higher content of the heterogeneous nucleation sites provided by TiC particles. Fig. 3(a) shows the OM image of the ϕ1 mm composite cylinders with 3 wt.% TiC particles. Small TiC particles and amorphous BMG matrix can be well distinguished. Fig. 3(b) shows the OM image of the ϕ3 mm composite cylinders with 3 wt.% TiC particles. The β-Ti dendrite with the size of about 8 μm nucleate around the blocky TiC particles. The outline of the β-Ti dendrite is sphere-like and distributed uniformly in the amorphous matrix. Fig. 3(c) shows the SEM backscattered image at a high magnification. The black contrast in the center region of the β-Ti dendrite came from the irregular *in situ* TiC particles. It implied that TiC particles act as the heterogeneous nucleation site for the β-Ti dendrite. The *in situ* TiC particles have a close interface bonding with β-Ti dendrite, which avoids the interface relaxation usually occurred in BMG composites. For ϕ4 mm BMG composite cylinders containing 5 wt.% *in situ* TiC particles shown in Fig. 3(d), the size of the β-Ti dendrite increases to be about 25 μm and the primary and second dendrite arm can be clearly observed. The volume fraction of the BMG matrix decreases further with the increment of the number and sizes of the β-Ti dendrites.

Since the Gibbs free energy of Ti+C→TiC reaction is of a great negative value, the *in situ* TiC particles can be formed even in the $Cu_{47}Ti_{34}Zr_{11}Ni_8$ alloy melts with a robust GFA. The precipitation of crystalline phase in the solidified alloy is the results of competing nucleation of the crystalline phase and the amorphous phase. If the time required for the crystalline phase to reach the critical nucleation rate is shorter than that of amorphous phase, the crystalline phase will precipitate first. Otherwise, the solidified alloy will keep in the amorphous state. The formation of *in situ* TiC particles increased the viscosity of the undercooled alloy melts, while provided more heterogeneous nucleation sites. Therefore, the presence of *in situ* TiC particles will increase the nucleation rate of the crystalline phase in the solidification process and make the crystalline phase precipitate from the undercooled alloy melts prior to the amorphous phase. It can be deduced that the TiC particles were formed in the undercooled alloy melts through the *in situ* reaction, then the β-Ti dendrite nucleated and grew around TiC particles in the subsequent

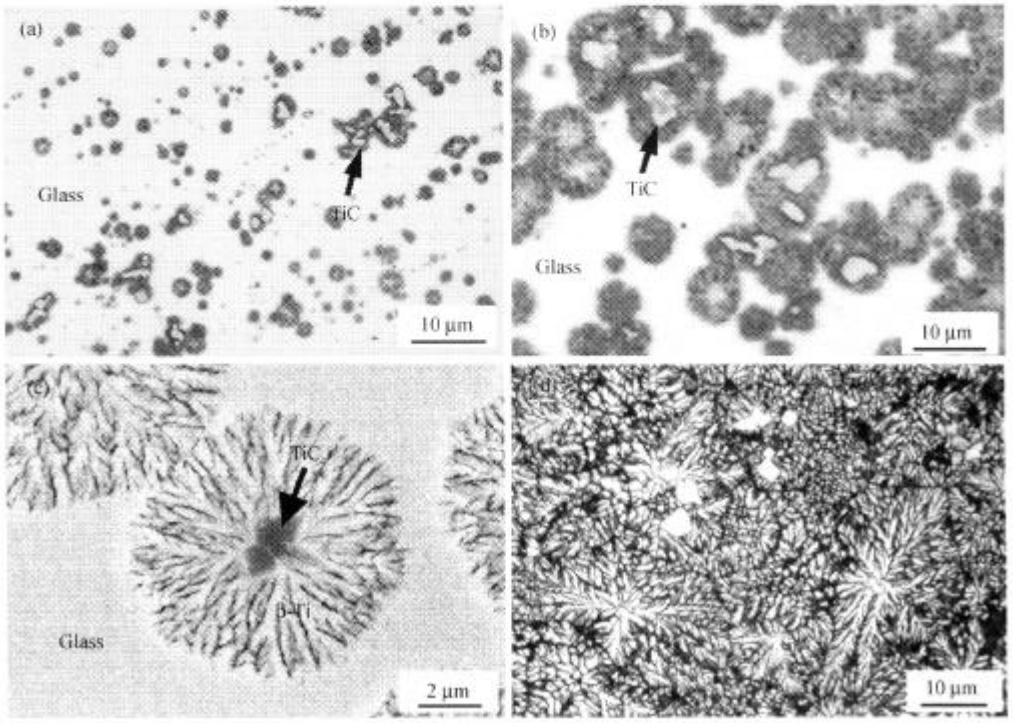

Fig. 3. Microstructure of TiC reinforced $Cu_{47}Ti_{34}Zr_{11}Ni_8$ BMG composite. (a) OM image of the ϕ1 mm composite containing 3 wt.% TiC; (b) OM image of the ϕ3 mm composite containing 3 wt.% TiC; (c) SEM backscattered image at high magnification; (d) OM image of the ϕ4 mm composite containing 5 wt.% TiC.

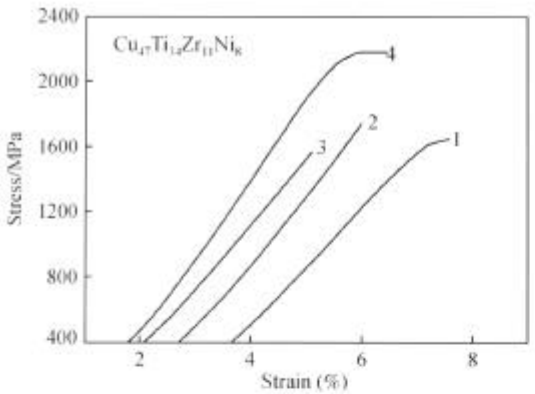

Fig. 4. Room temperature compressive stress-strain curves of $Cu_{47}Ti_{34}Zr_{11}Ni_8$ BMG composite sample (x represents the weight fraction of TiC). 1, x=1 wt.%, ϕ4 mm; 2, x=1 wt.%, ϕ3 mm; 3, x=0 wt.%, ϕ3 mm; 4, x=3 wt.%, ϕ2 mm.

cooling process. Finally, the remaining alloy melts were rapidly solidified into the amorphous matrix.

The room temperature compressive test was done on the composite cylinders. The stress-strain curve is shown in Fig. 4. It indicated that the mechanical properties of the BMG composite have some relationship with the size and the number of the reinforcements. For ϕ3 mm BMG composite sample containing only 1 wt.% TiC particles, the yield strength could be raised by 375 MPa. For ϕ4 mm BMG composite sample, the plastic strain could reach 0.25%. The yield strength and the plastic strain could even be raised to about 2300 MPa and 0.75% for ϕ2 mm composite sample containing 3 wt.% TiC particles. With the increase of weight fraction of the *in situ* synthesized TiC particles in the sample, the volume fraction of β-Ti dendrite was raised due to the increment of the nucleation sites, which cause a great enhancement of yield strength and ductility. However, a large amount of β-Ti crystalline would precipitate from the undercooled alloy melts and grew into coarse dendrites if the weight fraction of TiC particles increased to 5 wt.%. This induced the decrease of the volume fraction of the amorphous matrix in the sample and failure of high strength.

The plasticity of BMG alloys depends on the number of the shear bands appeared after plastic deformation[13,14]. For monolithic BMG alloy, only one or few highly localized shear bands are active and developed along the maximum stress direction before failure, which makes the BMG show little global plasticity. Shear bands were torn layer by layer along the direction of maximum stress and left the torn trace to vein patterns. But for BMG composites, the amorphous matrix will undertake most of the loading and will reach the elastic deformation limit quickly. The shear band then forms and expands to the reinforcements leading by the residual stress. The reinforcements deform plastically and interact with the formation and development of the shear bands in the matrix, which limits the propagation of the shear band around the reinforcements[15–18]. Dislocation motion, twinning and phase transformation induced plasticity are possible origins of plasticity of the dendrite, which is usually formed into network when acting with reinforcement. Dendrite deforms under loading and simultaneously transfers the loading to the surrounding glass matrix to promote the nucleation of multiply shear bands. The nucleated multiply shear bands propagate and interact with the arm of the dendrites. This hindered an isolated shear band to expand through the whole sample at the onset of plastic deformation and induced the sample deform homogeneously[19]. Fig. 5(a) shows the SEM image of the fracture surfaces of the ϕ2 mm monolithic $Cu_{47}Ti_{34}Zr_{11}Ni_8$ BMG after compressive deformation. It shows the typical vein pattern caused by the single shear band. Brittle rupture happens when the single shear band expands to some extent and forms a plain fracture surface. The local melting and the softened alloy, which look like liquid droplets formed under adiabatic rise in the deformation process, can also be observed on the fracture surface (indicated by the arrow in Fig. 5(a)). Fig. 5(b) shows the SEM image of the compressive fracture surface of the ϕ3 mm BMG compos-

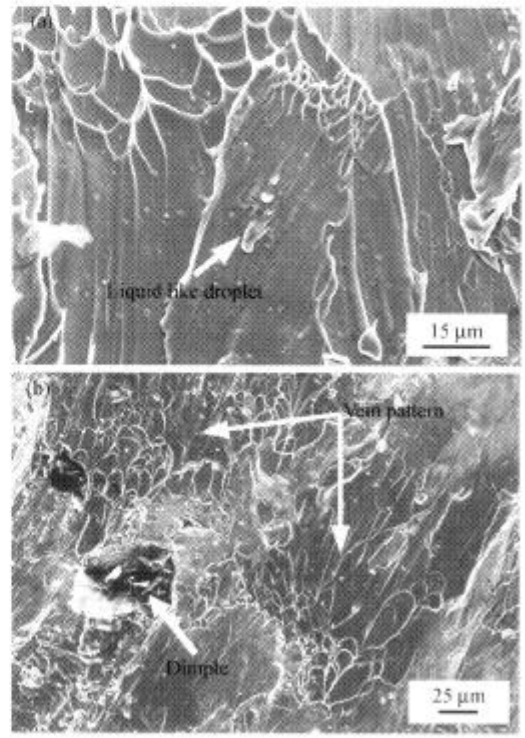

Fig. 5. SEM image of the compressive fracture surface of $Cu_{47}Ti_{34}Zr_{11}Ni_8$ BMG composites. (a) ϕ2 mm monolithic BMG alloy sample; (b) ϕ3 mm BMG composite sample containing 1wt% TiC particles.

ite sample containing 1 wt.% TiC. The white short arrows indicate the dimple caused by pull-out of the dendrite. Two individual shear bands can be observed above and below the dimple. So the formation of multiply shear bands prevent the inhomogeneous and highly localized deformation in the monolithic BMGs. The deformation behavior of the BMG composites is characterized by shearing of the glass matrix and dislocation motion in the dendrite. The failure is retarded by the interaction of shear bands and dendrite network.

3 Conclusions

TiC particles and β-Ti dendrite reinforced $Cu_{47}Ti_{34}Zr_{11}Ni_8$ BMG composites can be formed by the *in situ* reaction method. The presence of the *in situ* synthesized TiC particles could increase the thermal stability of the sample, while it has no influence on the GFA. In the meanwhile, the *in situ* synthesized TiC particles can act as the heterogeneous nucleation sites of β-Ti phase and promote the precipitation of the β-Ti dendrite. The number and size of the β-Ti dendrite increase with the increasing of the weight fraction of TiC particles or the increasing of the BMG composite cylinder diameter. Comparing with the monolithic BMG alloy, the propagation of single shear band was restricted in BMG composites. The compressive yield strength and ductility were improved due to the formation of multiple shear bands.

Acknowledgements This work was supported by the Knowledge Innovation Program of the Chinese Academy of Sciences (Grant No. KJCX2-SW-L05) and the National Natural Science Foundation of China (Grant No. 50101012).

References

1. Kawamura, Y., Shibata, T., Inoue, A., Deformation behavior of $Zr_{65}Al_{10}Ni_{10}Cu_{15}$ glassy alloy with wide supercooled liquid region, Appl. Phys. Lett., 1996, 69: 1208—1210.
2. Conner, R. D., Johnson, W. L., Shear bands and cracking of metallic glass plates in bending, J. Applied Physics, 2003, 94: 904—911.
3. Choi-Yim, H., Johnson, W. L., Bulk metallic glass matrix composites, Appl. Phys. Lett., 1997, 71: 3808—3810.
4. Fan, C., Li, C. F., Inoue, A., Nanocrystalline composites with high strength obtained in Zr-Ti-Ni-Cu-Al bulk amorphous alloys, Appl. Phys. Lett., 1999, 75: 340—342.
5. Eckert, J., Seidel, M., Kubler, A., Oxide dispersion strengthened mechanically alloyed amorphous Zr-Al-Cu-Ni composites, Scripta Materialia, 1998, 38: 595—602.
6. Eckert, J., Kubler, A., Schultz, L., Mechanically alloyed $Zr_{55}Al_{10}Cu_{30}Ni_5$ metallic glass composites containing nanocrystalline W particles, J. Applied Physics, 1999, 85: 7112—7119.
7. Kim, C. P., Busch, R., Johnson, W. L., Processing of carbon-fiber-reinforced $Zr_{41.2}Ti_{13.8}Cu_{12.5}Ni_{10.0}Be_{22.5}$ bulk metallic glass composites, Appl. Phys. Lett., 2001, 79: 1456—1458.
8. Fan, C., Ott, R. T., Hufnagel, T. C., Metallic glass matrix composite with precipitated ductile reinforcement, Appl. Phys. Lett., 2002, 81: 1020—1022.
9. Hays, C. C., Kim, C. P., Johnson, W. L., Improved mechanical behavior of bulk metallic glasses containing *in situ* formed ductile phase dendrite dispersions, Materials Science and Engineering, 2001, A304-306: 650—655.
10. Fan, C., Inoue, A., Ductility of bulk nanocrystalline composites and metallic glasses at room temperature, Applied Physics Letters, 2000, 77: 46—48.
11. Glade, S. C., Loffler, J. F., Bossuyt, S., Crystallization of amorphous $Cu_{47}Ti_{34}Zr_{11}Ni_8$, J. Applied Physics, 2001, 89: 1573—1579.
12. Lin, X. H., Johnson, W. L., Formation of Ti-Zr-Cu-Ni bulk metallic glasses, J. Applied Physics, 1995, 78: 6514—6519.
13. Jiang, W. H., Atzmon, M., The effect of compression and tension on shear-band structure and nanocrystallization in amorphous $Al_{90}Fe_5Gd_5$: A high-resolution transmission electron microscopy study, Acta Materialia, 2003, 51: 4095—4105.
14. Bian, Z., Chen, G. L., He, G., Microstructure and ductile-brittle transition of as-cast Zr-based bulk glass alloys under compressive testing, Materials Science and Engineering, 2001, A316: 135—144.
15. Choi-Yim, H., Conner, R. D., Szuecs, F., Processing, microstructure and properties of ductile metal particulate reinforced $Zr_{57}Nb_5Al_{10}Cu_{15.4}Ni_{12.6}$ bulk metallic glass composites, Acta Materialia, 2002, 50: 2737—2745.
16. Calin, M., Eckert, J., Schultz, L., Improved mechanical behavior of Cu-Ti-based bulk metallic glass by *in situ* formation of nanoscale precipitates, Scripta Materialia, 2003, 48: 653—658.
17. He, G., Eckert, J., Loser, W., Novel Ti-base nanostructure-dendrite composite with enhanced plasticity, Nature Materials, 2003, 2: 33—37.
18. Bian, Z., He, G., Chen, G. L., Investigation of shear bands under compressive testing for Zr-base bulk metallic glasses containing nanocrystals, Scripta Materilia, 2002, 46: 407—412.
19. Szuecs, F., Kim, C. P., Johnson, W. L., Mechanical Properties of $Zr_{56.2}Ti_{13.8}Nb_{5.0}Cu_{6.9}Ni_{5.6}Be_{12.5}$ ductile phase reinforced bulk metallic glass composite, Acta Mater., 2001, 49: 1507—1513.

(Received October 28, 2003; accepted December 4, 2003)